Outram, John G., Couperthwaite, Sara J., Bouzaid, Jocelyne, & Millar, Graeme J.
(2015)
Settling behaviours of low alumina/caustic ratios during seawater neutralisation of Bayer liquor. In
10th International Alumina Quality Workshop, 19-24 April 2015, Perth, Western Australia.

SETTLING BEHAVIOURS OF LOW ALUMINA/CAUSTIC RATIOS DURING SEAWATER NEUTRALISATION OF BAYER LIQUOR

John G. Outram[1], Sara J. Couperthwaite[1*], Jocelyne Bouzaid, Graeme J. Millar

[1] *School of Chemistry, Physics and Mechanical Engineering, Science and Engineering Faculty, Queensland University of Technology, Brisbane, Queensland, Australia*

Corresponding author: sara.couperthwaite@qut.edu.au

ABSTRACT

Factors that affect the settleability of seawater neutralised bauxite refinery residues are poorly understood, in particular, the settleability of precipitates in the absence of red mud and those formed with different alumina/caustic (AC) ratios. The influence of temperature, AC ratio, caustic concentration and the volumetric ratio of seawater on the settleability of seawater neutralisation precipitates and their respective compositions and stabilities have been determined. An array of techniques have been used to determine the composition and stability of precipitates and include pH, conductivity, inductively coupled plasma optical emission spectroscopy, infrared spectroscopy and X-ray diffraction. Temperature has been shown to have a significant influence on the settleability and calcium carbonate phase distributions in precipitates, as well as the overall stability of the precipitates. More complex phase compositions have also been found for Bayer liquors with lower AC ratios. The caustic concentration and temperature of the reaction have the greatest influence on the settling efficiency of the precipitates. Assessments on the chemical stability of the precipitates, precipitate settleability and discharge water quality have been made. In addition, productivity and environmental impacts caused by changes in precipitate settleability have also been considered.

1. INTRODUCTION

The seawater neutralisation of bauxite refinery residues reduces the pH to within discharge limits while simultaneously reducing dissolved metal concentrations (Palmer et al. 2008). Spent Bayer liquor alkalinity is neutralised through the precipitation of Mg, Ca and Al hydroxides and hydroxycarbonate minerals (Hanahan et al. 2004), in particular hydrotalcite ($Mg_6Al_2(OH)_{16}CO_3{\cdot}4H_2O$). Hydrotalcites are composed of positively charged layers of mixed hydroxides (brucite-like layer arrangement) with exchangeable anions between the positively charged layers.

Previous studies on hydrotalcite formation have focused on synthesis temperature (Cox and Wise 1995, Palmer and Frost, 2010, Palmer et al. 2008, Shirure et al. 2007) and characterisation (Frost et al. 2009, Hanahan et al. 2004, Palmer et al. 2008) of Bayer hydrotalcites, with little research on settling rates of hydrotalcites. Brucite ($Mg(OH)_2$) flocculation time and sedimentation (Petric 1980, Zhao et al. 2012) has been studied, while settling rates in the Bayer industry have been primarily focused on untreated red mud (Li and Rutherford, 1996).

Red mud has a highly variable composition that is dependent on the bauxite source. In untreated red mud, poor settling rates are generally caused by fine particles of iron oxides (Jones and Haynes 2011) and research has postulated that hematite rich mud settles faster than goethite rich mud. However, amorphous iron has been suggested to act as a bonding agent for red mud and synthetic flocculants (Li and Rutherford 1996). Most literature agrees with these statements, more or less determining that the effective surface area of the particles formed affect the settling rate (goethite has a much higher surface area than hematite) and the separation of solid-liquid mixtures is usually determined by the number of particles present, not the weight of the particles present.

This investigation aims to identify conditions in the seawater neutralisation process that promotes better settling of hydrotalcite and calcium carbonate precipitates.

2. EXPERIMENTAL

2.1 Materials

The Bayer liquor used was supernatant liquor (SNL), which was created from a real saturated evaporative liquid (SEL) with a Al_2O_3 concentration of 96g/L. Bayer liquor with known AC ratios were prepared by the dilution of SEL with known amounts of ultrapure water, sodium hydroxide (NaOH) and sodium carbonate (Na_2CO_3).

2.2 Experimental procedure

The apparatus was set up so that there was an appropriately sized reaction beaker and seawater (SW) feed beaker connected to a peristaltic pump. The SW pump tube was clamped to the side of the reaction beaker and the pH probe was calibrated to 7.00 and 10.00 before commencing the experiment. The seawater, sourced from Redcliffe, Queensland, Australia, was transferred to the seawater feed beaker, while the required amount of SNL was added to the reaction beaker.

The peristaltic pump rate for the AC and the low alumina experiments were set to 30 rpm and 270 rpm respectively. Firstly, once clear of any obstacles, the impellor was turned on at 200 rpm, and then the SW was pumped into the reaction beaker at 240 $mL.min^{-1}$. The pH of the solution was monitored until such time it reached the required pH or SW volume, a suspension sample was taken and the impellor was turned off.

2.3 Characterisation techniques

2.3.1 Settling rates

Two 100mL aliquots of the resultant suspension were added to separate Imhoff settling cones and the settling height of the precipitate was recorded at time intervals 3, 5, 10, 15, 30 and 60 minutes. The low alumina experiments (AC 0.05) had the settling height recorded at one minute intervals between time 0 to 10; five minute intervals between time 10 and 30; and 10 minute intervals between time 30 and 60.

1.3.2 X-ray diffraction (XRD)

X-ray diffraction patterns were collected using a Philips X'pert wide angle X-ray diffractometer, operating in step scan mode, with Co Kα radiation (1.7903 Å). Patterns were collected in the range 5 to 90° 2θ with a step size of 0.02° and a rate of 30s per step. Samples were prepared as Vaseline thin films on silica wafers, which were then placed onto aluminium sample holders.

2.3.3 Infrared spectroscopy

Infrared spectra were obtained using a Nicolet Nexus 870 Fourier Transform infrared spectrometer (FTIR) with a Smart Endurance single bounce diamond ATR (attenuated total reflectance) cell. Spectra over the 4000-525 cm^{-1} range were obtained by the co-addition of 128 scans with a resolution of 4 cm^{-1} and a mirror velocity of 0.6329 m/s.

2.3.4 Inductively coupled plasma – optical emission spectroscopy (ICP-OES)

Solutions were analysed using a VISTA-MPX CCD simultaneous ICP-OES instrument using an integration time of 0.15 seconds with 3 replications, with the following wavelengths: Al (396.152), Ca (422.673) and Mg (285.213). A certified standard from Australian Chemical Reagents (ACR) containing 1000mg/L of aluminium, calcium, magnesium, and sodium was diluted to form a multi-level calibration curve using a Hamilton Diluter.

3. RESULTS AND DISCUSSION

3.1 Effect of AC, caustic and temperature

The seawater neutralisation process typically occurs between 45 and 65°C due to the incoming hot Bayer liquor and ambient seawater streams. This elevated temperature will influence the kinetics and mineralogy of the reactions involved during neutralisation. In particular, the type of calcium carbonate ($CaCO_3$) that forms is greatly influenced by temperature, whereby, the less thermodynamically stable aragonite forms at temperatures above 40°C while stable calcite forms at room temperature (Wray and Daniels 1957). This investigation will look at what effect these mineralogical changes have on the settling performance of Bayer precipitates.

3.1.1 Settling rates

The settling rates of a range of Bayer liquors seawater neutralised to pH 9.37 at 25°C and 55°C are provided in Figure 1. At 25°C, the quickest precipitates to settle were produced from Bayer liquors with an AC ratio of 0.1

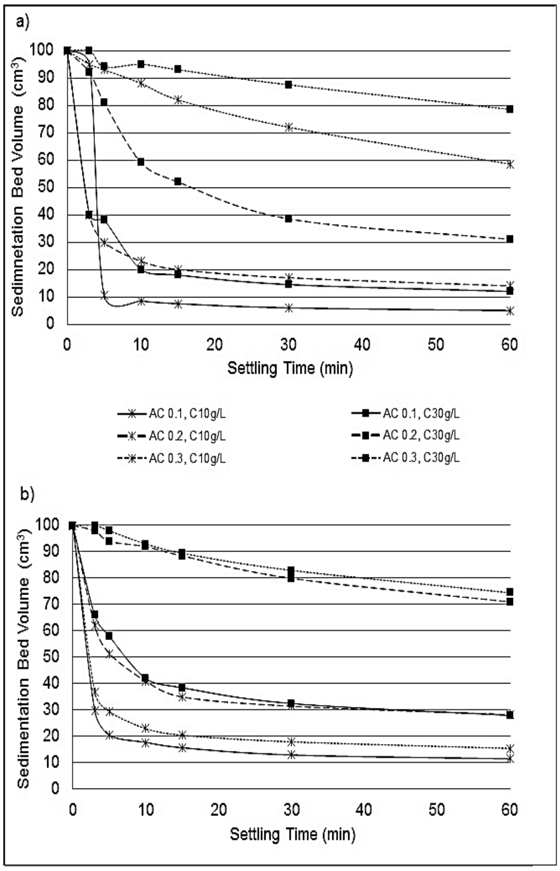

Figure 1: Settling rate of liquors neutralised to pH 9.4 at a) 25°C and b) 55°C

independent of the total caustic concentration. These precipitates showed hindered settling behaviour with stable bed volumes (<20cm^3) obtained within 20 minutes. It is observed that an increasing AC ratio at 25°C results in poorer settling, whereby precipitates formed with AC 0.3 liquors experience compression and hindered settling, and sedimentation bed volumes greater than 55cm^3. Higher aluminate concentrations allow for more hydrotalcite to form, which in turn results in a higher solids concentration per unit volume. Increasing the solids content per unit volume causes particles to interfere with one another causing settling rates to decrease. For all cases, precipitates formed from 10g/L caustic liquors had better settling qualities than those formed with 30g/L caustic liquors.

Increasing the temperature to 55°C showed the greater dependence of caustic concentration on settleability, with the lower caustic liquors producing precipitates with faster settling rates. Unlike the 25°C precipitates, the AC ratio does not appear to have the greatest influence on the type of settling experienced by the precipitates. For example, the AC0.2, C30g/L resulted in a sedimentation bed volume of 70cm^3 after 60 minutes compared to AC0.3, C10g/L with a sedimentation bed volume of 15cm^3. At increased temperatures it appears that the caustic concentration has the greatest influence on how the precipitates will settle. A similar observation has been made by Senaputra et al. 2013 who reported higher supernatant solids impeded settling. These precipitates predominately showed hindered settling, with some compression settling being observed for AC0.2, C30g/L and AC0.3, C30g/L samples.

The amount of seawater required to achieve a set neutralisation point decreased as the AC ratio increased independent of the neutralisation temperature (Table 1). Increasing the amount of available aluminate ions in solution increases hydrotalcite formation (primary driver behind reducing the pH through the intercalation of hydroxide ions (Rai, S. et al. 2013)), thus increasing the neutralisation efficiency of the process. Due to the lack of aluminate ions in AC 0.1 liquors the primary mode of pH reduction is a dilution effect caused by excessive amounts of seawater. The results show that a large number of particles in an enclosed area creates a slower-moving mixture. By increasing the volume of seawater required to neutralise the Bayer liquor there is less interference from other particles during the settling process and thus improves settling. Olsen and Direnga 1941 observed a similar trend for $CaCO_3$ sedimentation rates.

It is interesting to note that at 55°C there was no change in the seawater to Bayer liquor (SW:BL) ratio for Bayer liquors with an AC ratio of 0.2 and 0.3 independent of the caustic concentration. Palmer and Frost 2011 report that the interlayer spacing of hydrotalcite synthesised at 55°C is larger than those formed at room temperature. This larger spacing, along with the higher aluminium content, provides conditions for the intercalation of additional hydroxide ions.

ICP-OES results show that all aluminium has been removed from solution (Table 1) indicating that both reactions have reached completion. This is further confirmed by the pH levelling off after the rapid decline in the pH range 11.5 to 9.5. Previous studies have shown this rapid reduction in pH to be related

Table 1: Seawater to Bayer liquor volumes used to reach a neutralisation pH of 9.4

	25°C				
	SW:BL volume	**Mg (mg/L)**	**Al (mg/L)**	**Ca (mg/L)**	**Mg:Al ppt.**
AC 0.1, C10g/L	71.8:1	892	< 0.01	149	4.7:1
AC 0.2, C10g/L	13.6:1	783	< 0.01	206	3.4:1
AC 0.3, C10g/L	7.5:1	669	< 0.01	233	2.8:1
AC 0.1, C30g/L	69.4:1	772	< 0.01	212	4.6:1
AC 0.2, C30g/L	29.8:1	667	< 0.01	283	3.4:1
AC 0.3, C30g/L	15.6:1	163	0.3	201	2.6:1
	55°C				
AC 0.1, C10g/L	31.6:1	720	0.1	216	4.4:1
AC 0.2, C10g/L	6.0:1	248	< 0.01	26.6	3.2:1
AC 0.3, C10g/L	6.0:1	197	< 0.01	47.3	2.6:1
AC 0.1, C30g/L	31.7:1	638	0.1	216	4.5:1
AC 0.2, C30g/L	12.5:1	65.1	0.1	101	3.1:1
AC 0.3, C30g/L	12.6:1	13.3	0.8	79.0	2.5:1

to the formation of hydrotalcite and calcium carbonate species (Hanahan et al. 2004, Palmer and Frost 2011).

3.1.2 X-ray diffraction

The common mineralogical phases of the precipitates that form are hydrotalcite ($Mg_6Al_2(OH)_{16}CO_3{\cdot}4H_2O$), calcite ($CaCO_3$ – rhombohedral) and aragonite ($CaCO_3$ – orthorhombic). Variations in the relative amounts of each phase are observed for the different Bayer liquors used in this investigation (Figure 2). A lot of research has been conducted on the formation of the polymorphs of $CaCO_3$, including the influence of coexisting substances that act as growth inhibitors (magnesium) or stabilisers (strontium and barium) (De Choudens-anches and Gonzalez 2009, Saylor 1928, Wray and Daniels 1957, Zhang and Dawe 2000).

Precipitates formed at 25°C from AC 0.1 Bayer liquors have been observed to have the highest aragonite to calcite ratio, while an AC ratio of 0.3 showed a precipitate with predominately calcite. It is interesting to note that calcite is the only thermodynamically stable polymorph of calcium carbonate at room temperature (Reddy 1986) and yet it was formed in low AC conditions. The AC 0.1 liquors have higher ratios of Mg^{2+} to $Al(OH)_4^-$ in solution, which in turn results in higher respective Mg^{2+} concentrations when compared to the AC 0.2 and 0.3 solutions (Table 1). Lippmann 1973 has shown higher Mg^{2+} concentrations favour the precipitation of $CaCO_3$ as aragonite rather than calcite. Based on the work by Reddy 1986, it is proposed that aragonite is stabilised in solution due to Mg^{2+} inhibiting the dissolution-precipitation transformation of aragonite to calcite. A SEM image of a Bayer precipitate shows cubic-like calcite and circular aragonite structures embedded in a hydrotalcite particle (Figure 3). Elemental mapping of the particle confirmed the lighter areas of the image are calcium species, while a study by Andritsos et al. 1997 established the different morphologies of calcium carbonate.

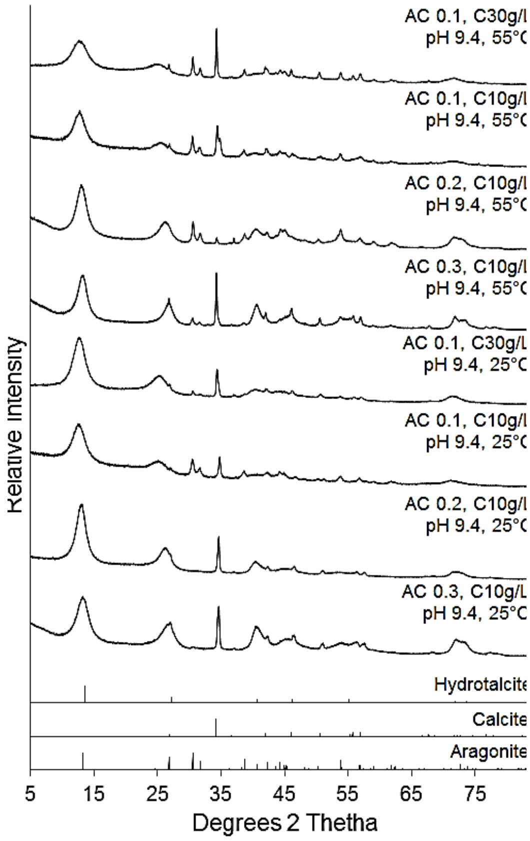

Figure 2: X-ray diffraction pattern of various Bayer precipitates

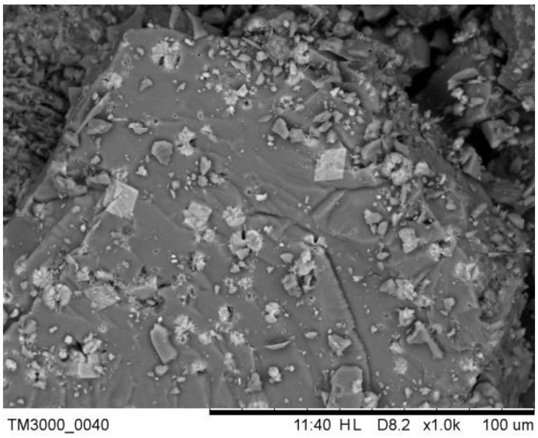

Figure 3: SEM image of $CaCO_3$ on a hydrotalcite particle

The distribution of calcium carbonate phases in the precipitates is shown to be mostly dependent on the reaction temperature. All of the 55°C samples showed increased amounts of aragonite, which agrees with literature that reports aragonite formation is favoured above 40°C (Burton and Walter 1987, De Choudens-Sanches and Gonzalez 2009, Sawada 1997, Saylor 1928, Wray and Daniels 1957). Even though the viscous resistance is lower in aragonite particles due to its di-pyramidal shape and smaller cross sectional area (increased sphericity) than calcite, it is not believed to be the overarching mechanism behind the improved settling rates.

Relating the XRD analysis to the settling rates of the AC samples, it can be seen that no compositional trend can be observed that correlates to the settling trends found earlier. Based on the results it is believed the main factor influencing the settling rates is the density of particles in a set volume of solution.

3.2 Effect of seawater neutralisation ratio

3.2.1 Settling behaviour

Increasing the amount of seawater added to Bayer liquor with an AC ratio of 0.05 and caustic concentration of 1 g/L shows a continual increase in settling rates (Figure 4). Three types of settling behaviours have been identified and include 1) compression settling (1:1 and 2:1), 2) hindered settling (3:1, 4:1 and 5:1) and 3) flocculation settling (10:1 and 20:1). The hindered and compression settling behaviours observed gave a clear sedimentation interface height or 'mud line', while flocculation settling did not. The flocculation settling observed for the 10:1 and 20:1 samples had a gradient solids concentration running the depth of the settling vessel.

The settling rates were determined as being the initial linear portion of the settling curves, after this point, the compression of the bed is observed which gives an inefficient sedimentation velocity. The settling velocity should effectively be thought of as the time taken to reach the 'compression point'. Settling velocities have been determined (Figure 4) for different SW:SNL ratios, all of which show acceptable regression fits of >0.98.

The 1:1 and 2:1 samples showed the poorest settling rates and exhibit compression and hindered/compression settling. The sedimentation bed volume of the 1:1 samples was around 65cm^3, while the 2:1 samples had a sedimentation bed volume of 45cm^3. These bed volumes are significantly higher than samples prepared using larger volumes of seawater. It is clear from Figure 4 that the rate of settling is not suitable for clarification purposes and is therefore not feasible. In addition, the pH obtained for these SW:BL

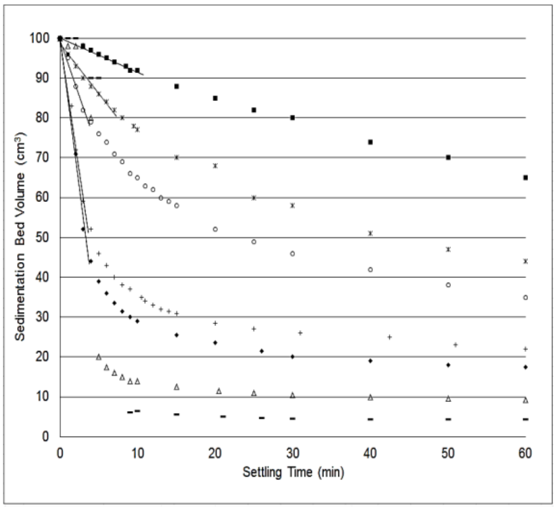

SW : SNL Ratio	Marker	Hindered Settling Velocity (cm³.min⁻¹)	Settling Behaviour Observed
1:1	■	0.9	Compression
2:1	⁎	2.4	Hindered/Compression
3:1	○	6.1	Hindered
4:1	+	12.6	Hindered
5:1	◆	15.6	Hindered
10:1	Δ	-	Free Floculation
20:1	▬	-	Free Floculation

Figure 4: Settling behaviour of Bayer liquor using varying volumes of seawater

Table 2: Elemental analysis of supernatants of set SW:BL volumetric ratios

SW:BL volumetric ratio	Supernatant properties				
	pH	Mg (mg/L)	Al (mg/L)	Ca (mg/L)	Mg:Al ppt.
1:1	10.35	139	1.7	9.6	3.8:1
2:1	9.96	368	< 0.01	11.6	4.5:1
3:1	9.75	637	< 0.01	15.0	4.7:1
4:1	9.67	911	< 0.01	16.3	4.7:1
5:1	9.56	1039	< 0.01	17.0	4.3:1
10:1	8.67	1201	< 0.01	39.8	3.8:1
20:1	8.12	1350	< 0.01	191	3.4:1

ratios is close to 10 (Table 2), which indicates that the SWN process has not completely neutralised the carbonate and caustic properties of the Bayer liquor (Hanahan, C., McConchie et al. 2004, Palmer et al. 2008). It is believed these two samples would exhibit secondary precipitation, however this has not been confirmed.

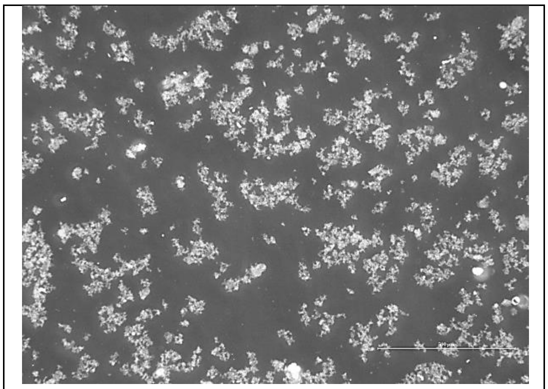

a) Ave size 277µm, Area 20%

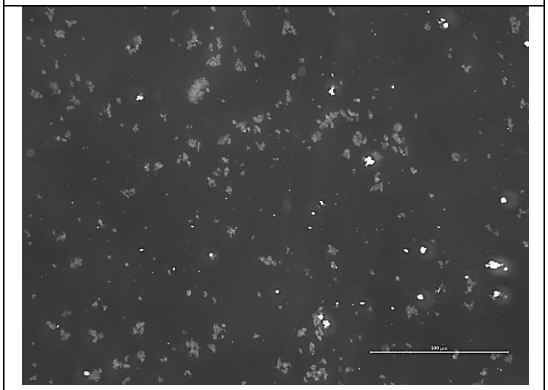

b) Ave size 93µm, Area 4%

Figure 5: ImageJ particle size analysis of optical images of flocs formed using SW:BL ratios a) 1:1, and b) 5:1

The 3:1 to 5:1 samples show the best parameters for neutralisation as there appears to be an acceptable trade-off between settling rate and type, and overall treated solution properties (pH, conductivity etc.). These 3 neutralisation products experienced hindered settling and produced a well-defined 'mud line' and clear supernatant within the 60 minute settling period. The majority of settling is completed within the first 20 minutes, while the rate limiting step occurs within the first 5-10 minutes. A linear regression was applied to the initial 5-10 minute step and is shown in Figure 4. It is clear from these results that increasing the volume of seawater used to treat a set volume of Bayer liquor will increase the settling rate of the precipitates. For example, the 3:1 neutralisation had a settling rate of $6.1cm^3$/min while the 5:1 increased to $15.6cm^3$/min.

The 10:1 and 20:1 showed free flocculation settling, this resulted in a poor 'mud line' or solid interface which caused issues with the supernatant clarity. These two samples were observed to have small flocs 'caught' in convection currents which refused to settle over the 60 minute period. Unfortunately, in order to obtain the desired pH for disposal these higher seawater volumes are required.

The settling rate for the 10:1 and 20:1 samples were not determined by the initial linear portion of the settling curve as these curves displayed different settling mechanics. These samples exhibited free flocculation settling where the colloidal particles destabilise, flocculate and fall through solution due to gravity. As the solution TSS concentration is low, the flocs do not experience hindrance when settling, thus once the flocs are large enough, the settling velocity is relatively fast until they have travelled the depth of the vessel and begin to experience compression setting. These curves (Figure 4) show an initial 'lag' period, where the particles destabilise and flocculate, followed by rapid decrease before finally plateauing.

3.2.2 Particle size

There are a number of factors that influence the settling rate of particles including 1) concentration of particles, 2) particle size, 3) density, 4) sphericity and 5) the viscosity of the fluid. Typically, smaller particles will settle a lot slower than larger particles, while very small particles can exhibit colloidal behaviour (Oursel et al. 2014). Agglomeration of particles has also been shown to increase settling rates due to their increased size. Figure 5 shows optical images (x3.2 magnification) of 1:1 and 5:1 precipitates formed and ImageJ values for the average size (µm) and solid area density (%).

The optical images clearly show the agglomeration of particles decrease as the volume of seawater is increased, resulting in much smaller dispersed solids. This is consistent with previous results that suggest the settling rates of the seawater neutralised precipitates are more dependent on the distribution of solids in solution than size of the particles or agglomerates that form.

3.2.3 X-ray diffraction

The XRD results show evidence of kinetic and thermodynamic changes occur as the volume of seawater increases (Figure 6). Initially, it appears that hydrotalcite is the kinetically favoured product (relative peak heights show it is the major phase in the 1:1 pattern). The addition of more seawater exhausts the amount of aluminium available to form hydrotalcite and the formation of calcium carbonate species begins to dominate the patterns. As previously observed, aragonite is dominant in these patterns even though these runs were completed at room temperature. This is due to the excess amount of magnesium in solution inhibiting the formation of calcite and the transformation of the unstable aragonite structure to calcite. Lastly, upon adding excessive amounts of seawater per unit volume of Bayer liquor, the crystallinity of hydrotalcite structure appears to improve.

Once again, no discernible trend in precipitate composition was found to correlate with the settling trends from Figure 4; further supporting that the settling of Bayer precipitates is predominately governed by the density of particles in a set volume of solution.

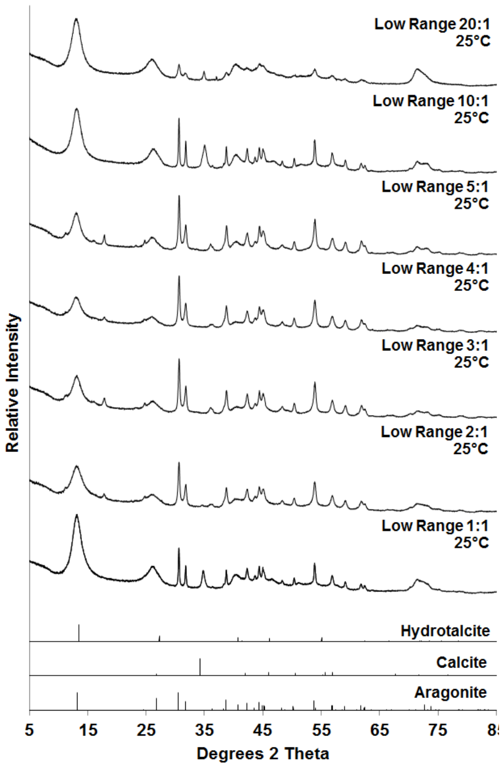

Figure 6: X-ray diffraction of Bayer precipitates formed with different volumes of seawater

4. CONCLUSION

The temperature, pH, AC ratio, caustic concentration and the volumetric ratio of seawater were shown to influence the settling behaviour of neutralised Bayer liquor. This study showed three types of settling behaviours: free flocculation, hindered and compression mechanisms.

It was found that decreasing the AC ratio of the Bayer liquors improved the settling rates due to the reduced amount of solids formed. Similarly, decreasing the caustic concentration of the Bayer liquors resulted in improved settling rates. Increasing the neutralisation temperature to 55°C showed a greater dependence on caustic concentration when compared to precipitates formed at 25°C; these predominantly showed hindered settling characteristics. The pH of the neutralised Bayer liquors was directly linked to the volumetric ratio of neutralisation, thus the pH was related to industry disposal requirements. The only neutralised sample that reached the desired pH of <9 was the 10:1 and 20:1 samples; which showed undesirable flocculation settling.

The volumetric ratio of the seawater to Bayer liquor was shown to have the greatest influence on the settleability of solids. This study revealed that the increasing volumetric ratio of seawater to Bayer liquor increased the settling rates of the precipitates due to the decreased particle distribution in the flocculations.

5. ACKNOWLEDGEMENTS

The financial and infra-structure support of the Energy and Process Engineering Discipline of the Science and Engineering Faculty and the Institute of Future Environments, Queensland University of Technology is gratefully acknowledged. The Australian Research Council (ARC) is thanked for funding some of the instrumentation used in this study (DE120101890). This study could also not have been completed without the support of the technical services team at QUT who ensured the analytical instrumentation was available to us.

6. REFERENCES

Andritsos, N., Karabelas, A.J. and Koutsoukos, P.G. 1997 Morphology and Structure of CaCO3 Scale Layers Formed under Isothermal Flow Conditions. Langmuir, 13, 2873-2879.

Burton, E.A. and Walter, L.M. 1987 Relative precipitation rates of aragonite and magnesium calcite from seawater: Temperature or carbonate ion control? Geology, 15, 111-114.

Cox, S.D. and Wise, K.J. 1995 Porous Spheroidal Hydrotalcite Aggregates. Mat. Res. Soc. Symp. Proc., 371, 151-156.

De Choudens-Sanches, V. and Gonzalez, L.A. 2009 Calcite and aragonite precipitation under controlled instantaneous supersaturation: elucidating the role of CaCO3 saturation state and Mg/Ca ratio on calcium carbonate polymorphism. J. Sediment. Res., 79, 363-376.

Farmer, V.C. 1974 The Infrared Spectra of Minerals. Mineralogical Society, London, 539 pp.

Frost, R.L., Spratt, H.J. and Palmer, S.J. 2009 Infrared and near-infrared spectroscopic study of synthetic hydrotalcites with variable divalent/trivalent cationic ratios. Spectrochim. Acta, Part A, 72A, 984-988.

Hanahan, C., McConchie, D., Pohl, J., Creelman, R., Clark, M. and Stocksiek, C. 2004 Chemistry of Seawater Neutralization of Bauxite Refinery Residues (Red Mud). Environ. Eng. Sci., 21, 125-138.

Jones, B.E.H. and Haynes, R.J. 2011 Bauxite Processing Residue: A Critical Review of Its Formation, Properties, Storage, and Revegetation. Crit. Rev. Environ. Sci. Technol., 41, 271-315.

Li, L.Y. and Rutherford, G.K. 1996 Effect of bauxite properties on the settling of red mud. Int. J. Miner. Process., 48, 169-182.

Lippmann, F. 1973 Minerals, Rocks, and Inorganic Materials: Monograph Series of Theoretical and Experimental Studies, Vol. 6: Sedimentary Carbonate Minerals. Springer, 228 pp. pp.

Olsen, J.C. and Direnga, O.G. 1941 Settling rate of calcium carbonate in the causticizing of soda ash. Ind. Eng. Chem., 33, 204-218.

Oursel, B., Garnier, C., Pairaud, I., Omanovic, D., Durrieu, G., Syakti, A.D. *et al.* 2014 Behaviour and fate of urban particles in coastal waters: Settling rate, size distribution and metals contamination characterization. Estuarine, Coastal Shelf Sci., 138, 14-26.

Palmer, S.J. and Frost, R.L. 2010 Thermal decomposition of Bayer precipitates formed at varying temperatures. J. Therm. Anal. Calorim., 100, 27-32.

Palmer, S.J. and Frost, R.L. 2011 Characterization of Bayer Hydrotalcites Formed from Bauxite Refinery Residue Liquor. Ind. Eng. Chem. Res., 50, 5346-5351.

Palmer, S.J., Frost, R.L. and Nguyen, T. 2008 Hydrotalcites and their role in coordination of anions in Bayer liquors: Anion binding in layered double hydroxides. Coordination Chemistry Reviews 253, 250-267.

Petric, B. and Petric, N. 1980 Investigations of the rate of sedimentation of magnesium hydroxide obtained from sea water. Ind. Eng. Chem. Process Des. Dev., 19, 329-335.

Rai, S., Wasewar, K. L., Lataye, D. H., Mukhopadhyay, J., Yoo, C. K. 2013 Feasibility of red mud neutralisation with seawater using Taguchi's methodology. Int. J. Environ. Sci. Technol., 10, 305-314

Reddy, M.M. 1986 Effect of magnesium ions on calcium carbonate nucleation and crystal growth in dilute aqueous solutions at 25°C. U.S. Geol. Surv. Bull, 1579, 169-182.

Sawada, K. 1997 The mechanisms of crystallization and transformation of calcium carbonates. Pure Appl. Chem., 69, 921-928.

Saylor, C.H. 1928 Calcite and aragonite. J. Phys. Chem., 32, 1441-1460.

Senaputra, A., Fawell, P., Jones, F. and Smith, P. 2013 Sodalite solids formation at the surface of iron oxide and its impact on flocculation. Light Met. (Hoboken, NJ, U. S.), 77-82.

Shirure, V.S., Nikhade, B.P. and Pangarkar, V.G. 2007 Intensification of Precipitation Using Narrow Channel Reactors: Case Study of Hydrotalcite Precipitation. Ind. Eng. Chem. Res., 46, 3086-3094.

Wray, J.L. and Daniels, F. 1957 Precipitation of calcite and aragonite. J. Am. Chem. Soc., 79, 2031-2034.

Zhang, Y. and Dawe, R.A. 2000 Influence of Mg2+ on the kinetics of calcite precipitation and calcite crystal morphology. Chem. Geol., 163, 129-138.

Zhao, J., Lin, W., Chang, Q., Liu, W., Wang, S. and Lai, Y. 2012 Effects of operational conditions on the floc formation time and rate in magnesium hydroxide coagulation process. Desalin. Water Treat., 45, 153-160.